

This is the author's final, peer-reviewed manuscript as accepted for publication (AAM). The version presented here may differ from the published version, or version of record, available through the publisher's website. This version does not track changes, errata, or withdrawals on the publisher's site.

Fourier transform infra-red spectroscopy using an attenuated total reflection probe to distinguish between Japanese larch, pine and citrus plants in healthy and diseased states

D.S. Gandolfo, H. Mortimer, J.W. Woodhall, and
N. Boonham

Published version information

Citation: Gandolfo, D et al. "Fourier transform infra-red spectroscopy using an attenuated total reflection probe to distinguish between Japanese larch, pine and citrus plants in healthy and diseased states". *Spectrochimica Acta Part A*, vol. 163 (2016): 181-188.

doi:[10.1016/j.saa.2016.03.022](https://doi.org/10.1016/j.saa.2016.03.022)

This version is made available in accordance with publisher policies under a Creative Commons **CC-BY-NC-ND** licence. Please cite only the published version using the reference above.

This item was retrieved from **ePubs**, the Open Access archive of the Science and Technology Facilities Council, UK. Please contact epubs@stfc.ac.uk or go to <http://epubs.stfc.ac.uk/> for further information and policies.

Title

Fourier Transform Infra-Red Spectroscopy Using An Attenuated Total Reflection Probe To Distinguish Between Japanese Larch, Pine and Citrus Plants In Healthy And Diseased States

Authors

Gandolfo DS*, Mortimer H

RAL Space
Science and Technology Facilities Council
Rutherford Appleton Laboratory
Harwell Oxford
Didcot
OX11 0QX
United Kingdom
Tel: +44 (0) 1235 445363

Woodhall JW, Boonham N

The Food and Environment Research Agency
Sand Hutton
York
YO41 1LZ
United Kingdom
Tel: +44 (0) 1904 462725

* Corresponding Author Email: daniel.gandolfo@stfc.ac.uk

Abstract

FTIR spectroscopy coupled with an Attenuated Total Reflection (ATR) sampling probe has been demonstrated as a technique for detecting disease in plants. Spectral differences were detected in Japanese Larch (*Larix kaempferi*) infected with *Phytophthora ramorum* at 3403 cm⁻¹ and 1730 cm⁻¹, from pine (*Pinus spp.*) infected with *Bursaphelenchus xylophilus* at 1070 cm⁻¹, 1425 cm⁻¹, 1621 cm⁻¹ and 3403 cm⁻¹ and from citrus (*Citrus spp.*) infected with 'Candidatus Liberibacter' at 960 cm⁻¹, 1087 cm⁻¹, 1109 cm⁻¹, 1154 cm⁻¹, 1225 cm⁻¹, 1385 cm⁻¹, 1462 cm⁻¹, 1707 cm⁻¹, 2882 cm⁻¹, 2982 cm⁻¹ and 3650 cm⁻¹. A spectral marker in healthy citrus has been identified as Pentanone but is absent from the diseased sample spectra. This agrees with recent work by Aksenov, 2014. Additionally, the spectral signature of Cutin was identified in the spectra of *Pinus spp.* and *Citrus spp.* and is consistent with work by Dubis, 1999 and Heredia-Guerrero, 2014.

Keywords

Bursaphelenchus xylophilus; Candidatus Liberibacter; Huanglongbing; Infrared, Phytophthora ramorum

1.0 Introduction

1.1 Plant Species and Diseases

Disease imposes a significant constraint on plant production. At least 10% of global food production is thought to be lost due to plant disease [1]. Plant diseases are also a constraint in forestry, amenity turf grass production, horticulture and can impact on the natural environment. For example non-native or introduced forest pathogens can have a significant impact on forest structure and composition [2]. The early detection and diagnosis of plant infections can allow effective disease management strategies to be implemented at an earlier stage than normal thus preventing proliferation of a plant disease.

In this study, we evaluated the use of FTIR spectroscopy for the detection of three pathogens that cause severe disease in their host plants: the oomycete *Phytophthora ramorum* in Japanese larch (*Larix kaempferi*), the nematode *Bursaphelenchus xylophilus* in *Pinus* species and the bacterium ‘*Candidatus Liberibacter*’ in *citrus* species.

P. ramorum is an invasive pathogen that causes ‘die-back’ and mortality in infected species [3] and at the time of writing it is listed in the UK plant health risk register as a quarantine disease. In 2009 it was discovered in Japanese larch trees in south west England. In 2010, the oomycete was found on larch trees in Wales, western Scotland and Northern Ireland [4] and by September 2012, 3 million Japanese larch trees had been felled in the UK in an attempt to bring the disease under control. Japanese larch is a commercially important wood that is used for boat building, fencing, garden furniture, wood biomass and more recently as a building material in construction.

Bursaphelenchus xylophilus is a plant parasitic nematode that causes ‘pine wilt’ primarily in *Pinus* spp. This disease results in tree death within a few weeks to a few months from infection [5]. The dead wood of all species of *Pinus* can act as a substrate for the development of *B. xylophilus*. The disease Citrus greening (or Huanglongbing) is caused by infection with ‘*Candidatus Liberibacter asiaticus*’, resulting in a reduced fruit crop yields and ‘die-back’ in citrus trees. Citrus greening has been widely reported in Africa, Asia and South America. The pathogen is primarily spread by two species of psyllid insect: the Asian citrus psyllid, *Diaphorina citri*, and the psyllid *Trioza erytreae*, which is present in Africa.

1.2 Spectroscopic Analysis of Plants Using Infra-Red Radiation

FTIR spectroscopy is an interferometric technique based upon the coherence of the superposition from the sample and reference beams of an interferometer. The raw data gathered by the detector of the instrument are Fourier transformed to extract the frequency dependent information. FTIR spectroscopy is a broad band technique that enables the study of plant material in the spectral range which coincides with the wavelength range of light which is highly reflected by leaves. The MIR spectral region, together with the far infra-red (FIR) region (25–1000 μm), is known as the molecular fingerprint region. At these wavelengths, rotational and vibration resonant couplings occur between chemical bonds within constituent molecules and the incident radiation. The use of other regions of the electromagnetic spectrum is limited by a number of factors. In the UV region (10–400 nm), solar radiation is strongly attenuated by chlorophyll and carotenoids, resulting in strong absorption. In the NIR region, high reflectance from the spongy mesophyll cells in the interior or lower part of the leaves results in the emergence of strong reflection rays. At shortwave infra-red (SWIR) wavelengths (1200–2500 nm), the response is strongly influenced by water content, cellulose and lignin concentrations, as well as several other biochemical constituents [6].

The frequencies of radiation that are attenuated by a sample relate directly to fundamental transitions in the atomic and molecular structure of the sample being probed. Vegetation is a complex target, as it has a large diversity of types, shapes and spatial distributions. There is great variation in molecular structure between different plant species and also between samples of the same species. The ratio and amount of absorption and reflectance of any biotic material is determined by the type, density, structure and vigour of the target. However, plant material containing chlorophyll is typically characterised by strong absorption in the visible wavelengths and high reflectance in the NIR range. In addition, leaf scale and pigment concentrations contribute to variations in absorption, transmittance and reflectance [6] from the leaf surface.

To date, the assessment of plant health using passive remote sensing methods has focused primarily on detecting either broadband thermal emission or specular and diffuse components of light in the ultraviolet (UV, 10–400 nm), visible (400–700 nm), near infra-red (NIR, 700–2500 nm) and mid infra-red (MIR, 2500–25000 nm) wavelengths [7]. Solar radiation provides a strong illuminating source within these spectral regions. The interaction between specific energies of light and plant material changes the characteristics of the reflected and transmitted radiation. These changes can be detected by a suitable detector, allowing the properties of the target sample to be inferred.

In this work we aim to test and develop optical methods to detect spectral differences between healthy and diseased plants. The following plants and diseases were studied: Japanese larch (*Larix kaempferi*) infected with *Phytophthora ramorum*, pine (*Pinus spp.*) infected with *Bursaphelenchus xylophilus* and citrus (*Citrus spp.*) infected with ‘*Candidatus Liberibacter*’.

2.0 Experimental Section

2.1 Plant Material Preparation

Phytophthora ramorum in Japanese Larch

Japanese larch trees approximately 1 m high were grown in a controlled environment room at 20°C, 50% relative humidity and on a 16:8 light: dark schedule. *P. ramorum* zoospores were prepared as described in [8]. The motility of the zoospores was verified using a microscope and their concentration was estimated to be 3000 zoospores per ml. Each larch tree branch was placed in a beaker containing 500 ml of zoospore suspension for 3 minutes. After this, each branch was covered with a plastic bag to increase humidity until symptoms (as visible sporangia on needles) were observed, up to 14 days later. The presence of *P. ramorum* was confirmed for each tree using lateral flow kits specific for *Phytophthora* species (Forsite Diagnostics Ltd, York, UK). Healthy samples were selected from plants which had not been inoculated or plants known to be disease free.

Bursaphelenchus xylophilus in Pine

Pinus sylvestris and *Pinus nigra* saplings (approximately 200 mm high) were kept in a quarantine glasshouse at 25°C. *Bursaphelenchus xylophilus* specimens were extracted from infested pine wood using the Baermann funnel technique. Nematode suspensions (containing 100 nematodes per μ l) were prepared and 25 μ l of this inoculum was injected into small incisions in the saplings approximately 50 mm above soil level. Wilting symptoms were seen in inoculated plants within 7–12 days. Healthy samples were selected from plants which had not been inoculated or plants known to be disease free.

‘*Ca. Liberibacter asiaticus*’ and ‘*Ca. Liberibacter africanus*’ in citrus

Shoots from citrus plants naturally infected with ‘*Ca. Liberibacter asiaticus*’ or ‘*Ca. Liberibacter africanus*’ were grafted onto healthy citrus plants and maintained in a glasshouse at 22°C and on a 16:8 light: dark schedule until symptoms of infection were observed on the host plants. Infected leaves were

separated from the host plants and stored at -20°C . The healthy samples of citrus were grown in a glasshouse space for several years before picking with no disease symptoms and which were known to be healthy.

2.2 Sampling Methodology

An FTIR spectrometer (Perkin Elmer Spectrum 100) incorporating an ATR probe was used throughout these tests. Light from an infra-red glowbar internal to the spectrometer was focused onto the ATR diamond crystal. The ATR method works by introducing infra-red radiation into a high refractive index crystal (in this case diamond) at an angle exceeding the critical angle of the crystal. The infra-red radiation is totally internally reflected at the interface angle where it is coupled to an external feature (in this case the leaf material) by an evanescent wave. The penetration depth of the evanescent wave varies with the wavelength of the incident radiation. (Figure 1) and penetrates to a depth of approximately $0.5\text{--}5\mu\text{m}$ into the substrate of the leaf. The evanescent wave is returned to the crystal and eventually exits the crystal and onto the detector. The transmission spectra of the ATR signal records the energy returning to the detector. In regions where the attenuation is less than 100% then the IR wave has been absorbed in the plant material. This is observed on an ATR attenuation spectra as less than 100%. Therefore transmissions approaching 0% mean that the energy at a particular wavelength has been absorbed. The penetration depth is also dependent upon wavelength and as the wavelength increases the penetration depth also increases.

The ATR method works by bringing a diamond crystal into full contact with the sample material. The crystal applies pressure to the sample to create a good contact for the evanescent wave to penetrate into the material. A greater applied force means that more energy is coupled to the sample and therefore more absorbance. This appears on an ATR transmission spectra to intensify a transmission peak. Additionally, the applied pressure can alter the chemistry of the sample and so shift the spectral peaks in wavelength. In this study we have used an identical applied force of the diamond on the sample as measured by the instrument for each measurement. Since the same pressure of the probe on the sample has been used for each measurement then the intensity of a spectral peak is proportional to the quantity of that chemical in a sample. A spectrum from the leaf material is calculated by using the Fourier Transform technique to extract spectral information from the interferogram.

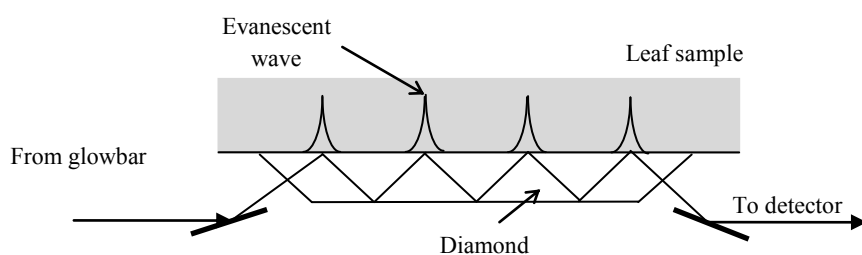


Figure 1. A diagram of the ATR unit with a diamond stage. The diamond is in full contact with the leaf material, which is pressed onto it from above. An evanescent wave penetrates into the leaf by a few microns and this attenuates the infra-red radiation that is directed towards the detector by a mirror.

The spectrometer was configured to collect spectra between 4000 and 500 cm^{-1} wavenumbers (2.5 μm and 20 μm) with a resolution of 4 cm^{-1} wavenumbers. This spectral range was chosen as it coincides with known spectral markers which have been observed in previous FTIR-ATR studies [9, 10, 11, 12, 13, 14, 15]. A lithium tantalite (LiTaO_3) non-cooled type detector was used. To enhance the signal-to-noise ratio (SNR) of each result, a total of 200 measurements were recorded and averaged to obtain a single spectrum. Instrument function artefacts were removed from the sample spectra by calculating a ratio of the spectra measured with no sample in the spectrometer beam line to that with a sample in the beam line. The resultant transmission spectra were further processed to automatically to remove the spectral features associated with the water/ CO_2 signal in the sample spectra.

In this study, errors occurred during data acquisition caused by background signal drifts which had the effect of giving false measurements, and in some cases demonstrated transmission spectra greater than 1 (i.e. a sample signal stronger than the background spectrum). The reason for this can be traced to instrumentation shifts due to temperature changes in the mirrors, detectors, beamsplitter and electronics. To prevent this, background spectra were taken at regular intervals (every 2–3 hours). Measurements in the spectrometer were related to atmospheric conditions such as changes in the humidity and gas (H_2O and CO_2) content of the air. To counter this, the spectrometer software efficiently removed H_2O and CO_2 spectral signals.

To assess the accuracy and repeatability of the measurement technique, repeat measurements were made of pine samples infected with *Bursaphelenchus xylophilus*. A healthy pine needle was placed in the ATR unit and seven measurements were made at regular time intervals, with each measurement taking approximately 1 minute. The measurements were carried out without adjusting the ATR unit. It was found that there was a progressive decrease in the attenuation of approximately 2.5% at the peak wavelengths in three regions of the spectrum (650–900 cm^{-1} , 1600–1670 cm^{-1} and 3000–3700 cm^{-1}). Additionally, the absorption peaks at 719 cm^{-1} , 1163 cm^{-1} , 1733 cm^{-1} , 2848 cm^{-1} and 2915 cm^{-1} had

minimal errors in wavelength and absorption percentage shift. When multiple measurements were made on a single pine needle along its whole length, absorption percentage errors were seen. The same peaks constituting a whole spectrum were observed at 719 cm^{-1} , 1163 cm^{-1} , 1733 cm^{-1} , 2848 cm^{-1} and 2915 cm^{-1} with minimal wavelength shifts. In this case, however, there was an average random change of 18.1% in absorption at these peaks. A second pine needle was measured and these measurements demonstrated an average absorption percentage change of 21.0%. The same peaks were observed with very little wavelength shift between samples. Overall, these tests demonstrated that this experimental method is very good at identifying prominent peaks in a sample with wavelength shifts of the order of $1 - 3\text{ cm}^{-1}$ between like samples. However, the absorption magnitude of these peaks is subject to drift by an average of 19.5% across multiple measurements.

3.0 Results

The spectra are convolved FTIR interferograms whereby 100% equates to 100% transmission and 0% equates to 100% absorption of the radiation in the plant sample. The data shown have not been adjusted and are raw transmission spectra whereby the spectra equals sample spectra divided by the background spectra. The only post-processing which has been carried out is to reduce the $\text{H}_2\text{O}/\text{CO}_2$ signal at approximately 2300 cm^{-1} . The spectra are measurements from a single sample of either a healthy or diseased plant leaf or needle. Each measurement is self calibrated to a Nd:YAG (1064 nm) laser within the spectrometer to provide accurate wavelength data. To emphasise the spectral differences between the healthy and diseased spectra, the infected spectra have been subtracted from healthy spectra and these are shown on the graphs with the y-axis legend 'Healthy – Infected'. By subtracting the diseased spectra from the healthy spectra differences between the two spectra will emerge. The differences between healthy and diseased spectra reveal chemical changes which have occurred in the plant due to infection.

Phytophthora ramorum on larch

Figure 2 shows a spectrum from a healthy Japanese larch needle compared with one from a Japanese larch needle infected with *P. ramorum*. The notable difference between the two spectra is the peak at 1733 cm^{-1} which does not appear on the healthy spectra but only appears on the diseased spectra. Figure 2b shows the subtraction of the infected spectrum from the healthy spectrum to highlight the spectral differences. The peaks at 2914 cm^{-1} and 2851 cm^{-1} are more intense in the diseased spectra and the broad peak at 3403 cm^{-1} is less intense for the diseased spectra.

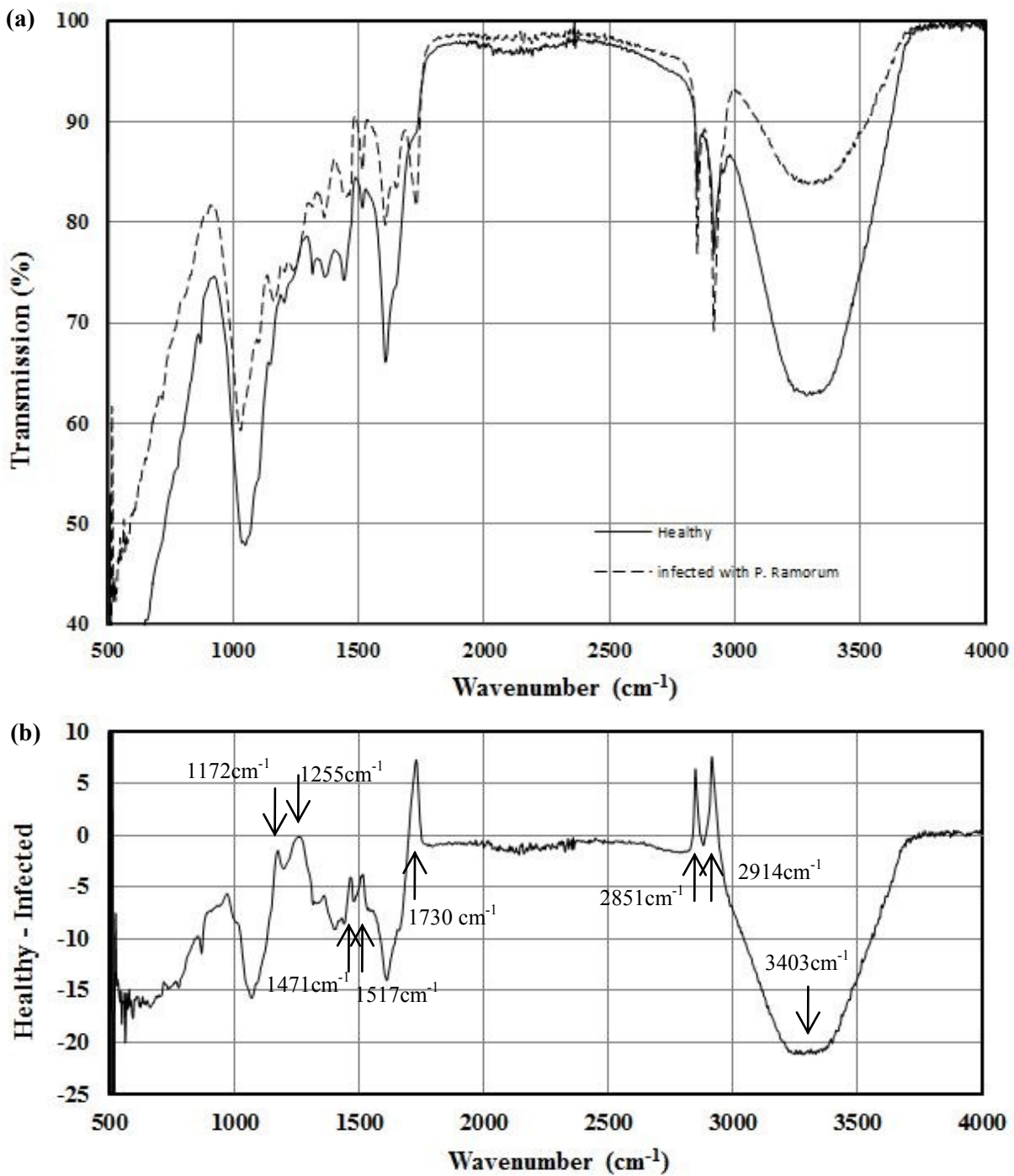


Figure 2. FTIR-ATR data from Japanese larch needles. (a) Spectra from a healthy Japanese larch needle and a *P. ramorum* infected larch needle are shown. (b) Subtraction of the diseased spectrum from the healthy spectrum reveals the significant peaks. The arrows indicate notable differences between the two spectra.

Bursaphelenchus xylophilus on pine

Pine needles were analysed using the FTIR spectrometer with the ATR sampling probe. Figure 3 shows a spectrum from a healthy pine needle compared with a spectrum from a pine needle infected with pinewood nematode (*Bursaphelenchus xylophilus*). Figure 3b shows the subtraction of the infected

spectrum from the healthy spectrum to highlight the differences in the spectra. The peaks at 1070 cm^{-1} , 1425 cm^{-1} and 1621 cm^{-1} are identified as peaks present in the healthy spectra but are absent in the diseased spectra. The broad peak identified at 3403 cm^{-1} is less intense in the infected spectrum than the healthy spectrum.

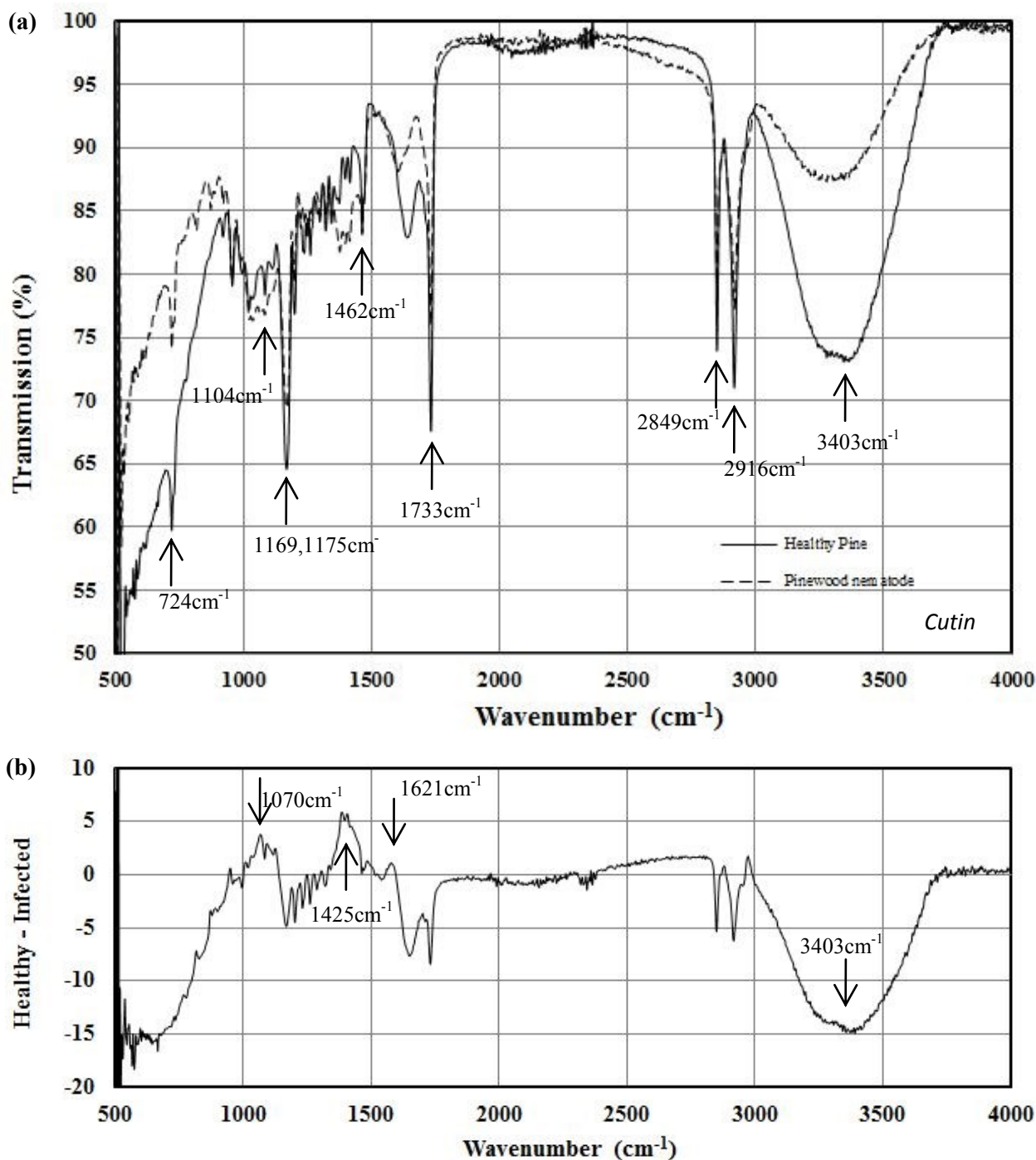


Figure 3. FTIR-ATR data from pine needles. (a) The spectra from healthy pine needles and pine needles infected with pinewood nematode (*B. xylophilus*). The spectral lines indicated collectively identify cutin.

(b) Subtraction of the diseased spectrum from the healthy spectra. The arrows indicate differences between the two spectra.

‘Ca. Liberibacter’ in citrus

Citrus leaves were analysed using the spectrometer with the ATR sampling probe. Figure 4 shows the spectrum from a healthy citrus leaf compared with spectra from two citrus leaves with *citrus greening* (infected with ‘Ca. Liberibacter asiaticus’ and ‘Ca. Liberibacter africanus’). The differences between the healthy and diseased spectra are at 960 cm⁻¹, 1087 cm⁻¹, 1109 cm⁻¹, 1154 cm⁻¹, 1225 cm⁻¹, 1385 cm⁻¹, 1462 cm⁻¹, 1740 cm⁻¹, 2882 cm⁻¹, 2982 cm⁻¹ and 3650 cm⁻¹. The subtraction spectra (Figure 4b) clearly show these differences.

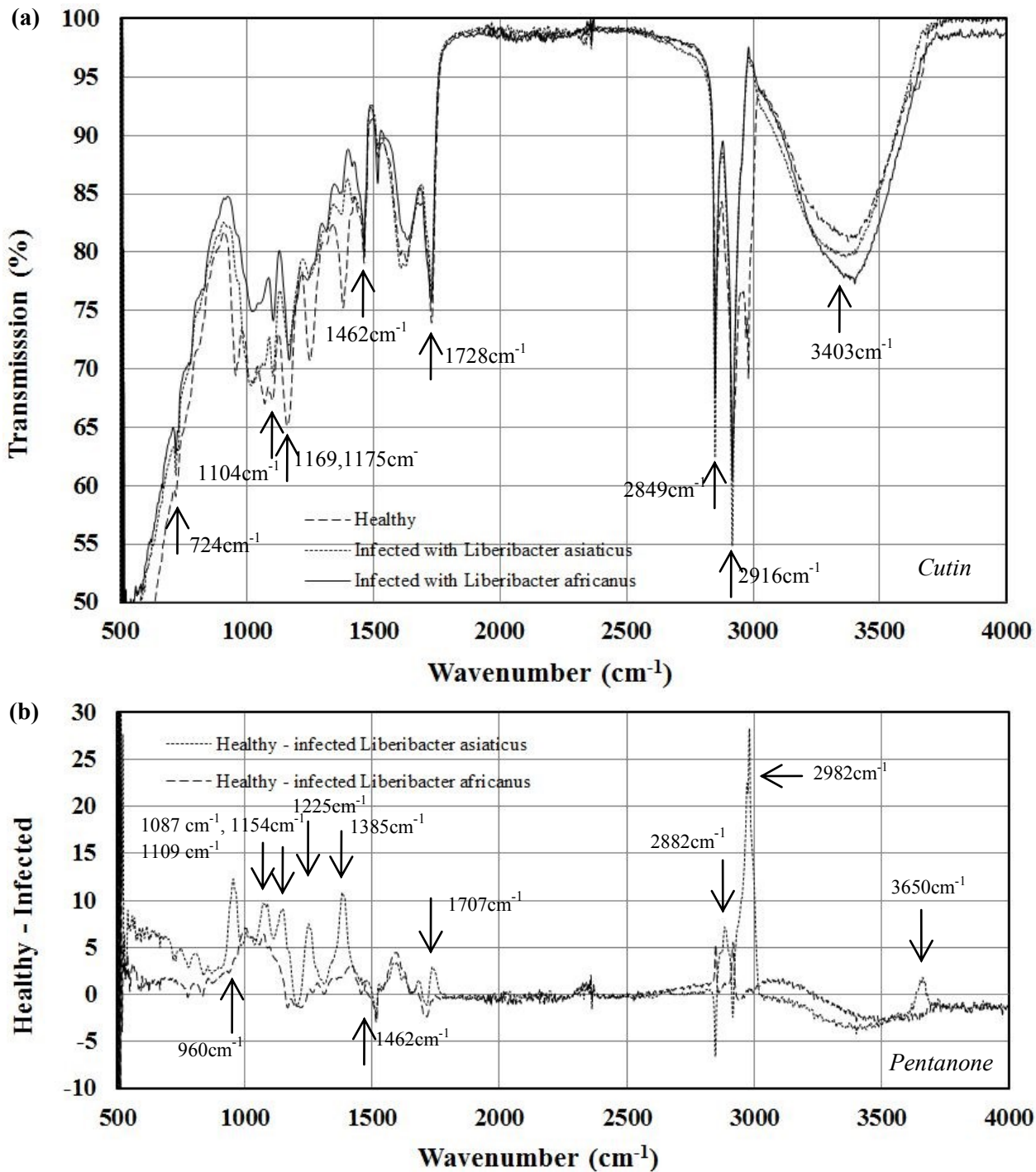


Figure 4. ATR spectra from citrus leaves. (a) Spectra from a healthy citrus leaf and from citrus leaves infected with citrus greening ‘Ca. *Liberibacter asiaticus*’ or ‘Ca. *Liberibacter africanus*’ are shown. The arrows show differences between the three spectra. Highlighted peaks are the spectral markers for Cutin in the healthy sample. (b) Subtraction spectra (healthy *Liberibacter asiaticus* - infected and healthy *Liberibacter africanus* - infected). Assigned peaks are the spectral markers for 3-Pentanone.

Aksenov [16] carried out an extensive study on Huanglongbing infected citrus samples. They analysed the diseased plants using gas chromatography / mass spectroscopy and identified a multitude of volatile organic compounds (VOCs) emanating from the diseased plants. One of the VOCs was pentanone. In this

study we have matched the transmission peaks of the spectrum of pure 3-pentanone ($C_5H_{10}O$) [17] (Figure 5) with the healthy Citrus transmission peaks. When only the 1728 cm^{-1} , 2916 cm^{-1} and 2982 cm^{-1} peaks between 1665 and 3019 cm^{-1} on the healthy Citrus and 3-Pentanone spectra are considered, the correlation between the two is > 0.9 indicating a very good fit (1.0 indicates a perfect correlation between two data-sets, -1.0 indicates an inverse correlation and 0.0 indicates zero correlation). The correlation function is defined as:

$$\text{Correl}(X, Y) = \frac{\sum(x-\bar{x})(y-\bar{y})}{\sqrt{\sum(x-\bar{x})^2 \sum(y-\bar{y})^2}}$$

Where X is the healthy citrus data set and Y is the matched 3-Pentanone data-set at each wavenumber. The healthy citrus data set was normalised to the pure 3-Pentanone data-set using Bruker Opus and Microsoft Excel software. Normalisation was carried out as follows. Two curves were fitted to the data in the wavenumber regions of 750 to 1664 cm^{-1} and 2920 to 3700 cm^{-1} . The data were then adjusted to remove the peak at 3403 cm^{-1} (hydroxyl) and the downward trend in the healthy citrus data in the wavelength region 750 to 1664 cm^{-1} was shifted towards the baseline at 100% transmission. The resulting spectrum is shown below in Figure 5 plotted with the pure 3-Pentanone data-set [17]. The correlation between the data-sets in the wavelength region 1000 cm^{-1} to 3700 cm^{-1} was calculated as 0.757 indicating a high correlation between the data.

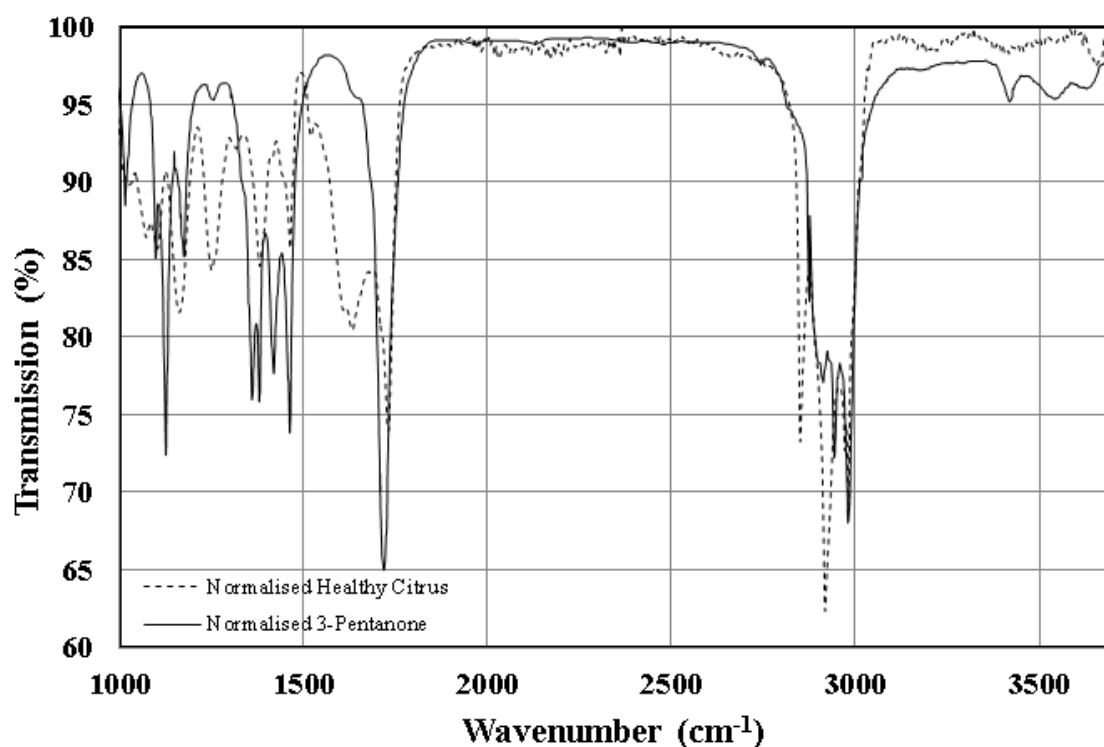


Figure 5. Normalised data-sets for healthy Citrus and 3-Pentanone [16] to emphasise the matching transmission peaks and to calculate the mathematical correlation between the two data-sets.

The peak at 2982 cm⁻¹ is not a single peak and this is matched to the spectrum of pentanone which has three peaks at 2979 cm⁻¹, 2941 cm⁻¹ and 2908 cm⁻¹. Additionally, the highlighted peak at 1154 cm⁻¹ is actually two peaks and can be matched to the 3-pentanone spectrum at 1172 cm⁻¹ and 1122 cm⁻¹. The healthy citrus peak at around 1730 cm⁻¹ is actually a double peak. So the secondary peak at 1707 cm⁻¹ can be assigned to pentanone and the peak at 1731 cm⁻¹ can be assigned to cutin. The transmission peaks of 3-Pentanone can be matched with the transmission peaks of the healthy spectrum of *Citrus spp.* shown in Figure 4a but the Pentanone spectrum is absent from the infected citrus spectrum and this is clearly demonstrated in Figure 4b. Table 1 below shows the matched transmission peaks between the healthy citrus spectrum and the 3-Pentanone spectrum.

Figure 4 Peaks (cm⁻¹)	3-Pentanone [ref. 22] Peaks (cm⁻¹)
3650	3638, 3416
2982 (multi-peak)	2979, 2941, 2908
2882	2884
1707	1716
1462	1461, 1415
1385	1369
1225	1250
1154	1172, 1122
1087, 1108	1096
960	957

Table 1. Spectral peaks shown in Figure 4b matched to the spectral peaks for 3-pentanone [21].

4.0 Discussion

FTIR spectroscopy with the ATR method has been used in the past to study different types of plant material including tobacco and horse chestnut. Ivanova [10] used FTIR with an ATR probe to examine leaf senescence and ageing of plant material. At 1500–1650 cm⁻¹, they found differences in the spectra of young leaves and old leaves of both black cherry and sweet pepper bush plants, indicating a higher relative concentration of phenolics in the older leaves. In addition, tobacco leaves under prolonged physiological stress exhibited a progressive, time-dependent increase in absorbance at around 3475 cm⁻¹, corresponding to a hydroxyl functional group. The work here also observed changes in the hydroxyl group at 3475 cm⁻¹ showing a broad peak (+/- 400 cm⁻¹) centred around 3400 cm⁻¹ for each spectra. In this study the needle structured plants (Japanese Larch and *Pinus spp.*) demonstrated significant differences between healthy and diseased samples but the leaf structured plant (*citrus spp.*) did not.

Hawkins [11, 12] used FTIR with an ATR probe to distinguish between healthy citrus and citrus infected with Huanglongbing. The largest difference between healthy and diseased plants occurred in the spectral region 900-1150 cm^{-1} and was centred on 1020 cm^{-1} . They developed a chemometric model based on the spectra of 179 plants. The model was able to predict from a given spectra with >95% confidence if the plant was diseased or not. They assigned the region of 900 – 1150 cm^{-1} to carbohydrate vibrational bands with various sugars, starches and cellulose. A key change with a Huanglongbing infection is that the fruit becomes small, light and very acidic. The acidity may be largely due to a change in the carbohydrates present and this was detected in the spectra. The work here also detected changes between healthy and diseased citrus plant samples centred at 1000 cm^{-1} within the range +/- 200 cm^{-1} .

FTIR coupled with ATR has been shown to be a powerful tool for identifying plant disease in work by Da Luz [18]. He demonstrated that it is possible to correctly identify tree species using FTIR-ATR spectroscopy with reference to ATR data libraries. He used 117 individual samples with 32 different tree species. 83% were correctly identified. He used a spectral search algorithm with reference to ATR data libraries. The work demonstrated a number of things including spectral differences between sun exposed and sun deprived leaves, spectral differences between young and old leaves of the same species, and that the spectral features of leaves of *Olea europaea* can be broken down into constituent parts using computer simulations. The work identified a multitude of compounds in plants with reference to their spectral features. He also states that because plants contain many organic compounds and produce complex spectra, it is currently not possible to definitively identify each constituent from its spectra. At present, the collection of spectra of pure plant constituents measured by ATR is few and far between.

Dubis [19] carried out a comparative study using FTIR-ATR on different plant leaves and needles (Potato leaf, Geranium leaf, Wandering Yew leaf, Yew-Tree needle and Spruce needle). They identified that there were significant similarities in the spectra between these species. The leaves analysed from the different species had different thicknesses of waxy cuticle and this was reflected in the spectral peak intensity. In actual fact, the spectral peaks identified in the Dubis [19] work were all present in the spectra of Pine needles (Figure 3a) and Citrus (Figure 4a) but not the Japanese larch spectra. The peaks at 1728 cm^{-1} , 1462 cm^{-1} , 1175 cm^{-1} , 1169 cm^{-1} and 1069 cm^{-1} are missing from the healthy Japanese larch spectra. Work by Heredia-Guerrero [20] identified the same spectral peak group to be characteristic of cutin, a predominant component of the plant cuticle matrix. This layer is directly below the waxy epicuticular layer of plant surfaces. The data from Dubis [19] and Heredia-Guerreo [20] for cutin has been combined in Table 2 and shows the designations for the spectral peaks seen in Figures 3 and 4.

Wavenumber (cm ⁻¹)	Assignment	Description
3403	ν OH	hydroxyl
2916	ν_{asym} CH ₂	methylene
2849	ν_{s} CH ₂	methylene
1728	ν C=O	ester
1462	δ_{s} CH ₂	methylene
1175	ν CH ₂ -O-CO	ester
1169	ν_{asym} C-O-C	ester
1104	ν_{s} C-O-C	ester
724	δ CH ₂	methylene

Table 2. Spectral peaks characteristic of Cutin identified in Figures 3 and 4. Data from Dubis, 1999 and Heredia-Guerreo, 2014.

Plešerová [13] used FTIR-ATR spectroscopy to study Norway spruce needles. Spectral peaks at 2915 cm⁻¹, 2848 cm⁻¹, 1732 cm⁻¹, 1464 cm⁻¹ and 1166 cm⁻¹ coincided with peaks seen in this study for Pine needles and Citrus leaves but not for Japanese larch needles. These spectral peaks were assigned to the cuticle waxes on the surface of needles. They found that the spectra obtained from each needle were not dependent upon where along the needle the measurement was made. They also found that an optimal fixation pressure on the needle by the ATR crystal is required to obtain reliable spectra without damaging the needle surface.

For the study here, Figure 2 (Japanese Larch) does not show evidence for a complete spectrum for cutin as shown in the spectra for *Pinus spp.* (Figure 3) and Citrus (Figure 4). For the diseased spectra of Japanese Larch a peak appears at 1733 cm⁻¹ and the two peaks at 2914 cm⁻¹ and 2849 cm⁻¹ are more intense. The peak at 1733 cm⁻¹ can be assigned to ν C=O for ester which is a constituent of the plant cuticular matrix [19, 20].

From the three plant types, *Pinus spp.* (Figure 3) shows the least difference between healthy and diseased spectra. The broad peak centred at 3403 cm⁻¹ demonstrates a difference of 15% between healthy and diseased samples. The peak has been assigned to hydroxyl. The peaks shown in Figure 3b at 1070 cm⁻¹ (cuticular wax), 1425 cm⁻¹ (cuticular wax) and 1621 cm⁻¹ (phenolic compounds) have been identified previously by Trebolazabala [23]. They used Confocal Raman Spectroscopy in assigning molecular identifications to spectral peaks. The spectral fingerprint of cutin is clearly evident in the healthy spectrum of pinus (Figure 3a).

Figure 4 presents an important difference in the spectra between healthy and infected citrus leaf samples. The lines at 3650 cm^{-1} , 2982 cm^{-1} , 2882 cm^{-1} , 1707 cm^{-1} , 1462 cm^{-1} , 1385 cm^{-1} , 1225 cm^{-1} , 1109 cm^{-1} , 1087 cm^{-1} , 960 cm^{-1} in the healthy citrus leaves are indicative of pentanone [17] which is a known constituent of citrus plants [22]. Work by Aksenov [15] in which they carried out an extensive chemical analysis on the released volatile organic compounds (VOCs) in citrus infected with Huanglongbing, found that pentanone (as well as a multitude of other compounds) was released from the leaves with the plant infected with Huanglongbing but had a much weaker detection rate in the healthy plants. This meant that pentanone was being retained in the leaves of healthy plants. They measured the VOCs to fingerprint biomarkers using the analytical methods of gas chromatography and differential mobility spectrometry. Therefore, pentanone is retained in the healthy citrus leaves which was detected by the ATR experiment in this study. In the diseased citrus leaves the pentanone is not present (as shown by the Aksenov experiment) therefore it can be inferred to some extent that pentanone is released from the citrus leaves when the plant is infected with Huanglongbing.

Figure 5 shows the normalised data for healthy citrus shown against normalised data for 3-Pentanone. The infra-red spectrum of 3-pentanone was acquired from a pure liquid sample of 3-Pentanone whereas the leaf spectrum acquired from a healthy leaf has within it markers not just from 3-Pentanone but includes other components such as hydroxyl with a peak at 3403 cm^{-1} . The two peaks at 1254 cm^{-1} and the double peak at 1636 cm^{-1} in healthy citrus on Figure 5 remain unidentified. The correlation of normalised healthy citrus and normalised 3-pentanone gives a value of 0.757 indicating that the spectrum of pure 3-Pentanone is contained within the spectrum of healthy Citrus. The 3-Pentanone spectrum is not contained within the diseased citrus spectrum and this corroborates work by Aksenov [16].

In the present study we have shown that FTIR-ATR can distinguish between the spectra of healthy and diseased plant samples in Japanese larch (*Larix kaempferi*), pine (*Pinus* spp.) and citrus (*Citrus* spp.). The measurement technique is straightforward to set-up requiring a background scan and then a sample scan. The final spectrum calculation was then carried out automatically by computer. The total time taken for the complete procedure was approximately 10 - 15 minutes making this a fast method to test multiple plant samples for disease. With further work it is a promising method for quick and easy identification of disease. Additionally, spectrometers have now been miniaturised to such an extent that they are used in-the-field for plant based applications [21].

To improve future measurements, more repeat data will be recorded for each sample to reduce experimental error and this will determine exemplar diseased and healthy spectra. Additionally, it will be possible to obtain better data when detectors with optimal responses in the spectral regions of interest

become available. Furthermore, because the detector functions at its best when the signal is high and the noise is low, improvements in optics that allow more light to reach the detector will facilitate the achievement of better measurements with good signal-to-noise ratios.

5.0 Conclusion

This spectroscopic study was carried out to assess the feasibility of using FTIR spectroscopy with an ATR probe to differentiate between healthy and diseased plant samples. The experiments have shown that it is possible to differentiate between the spectra of healthy and diseased Japanese larch, pine and citrus species. In the spectrum from the diseased Japanese larch sample, a prominent line appeared at 1733 cm^{-1} which was not present in the spectrum from the healthy larch sample. For *Pinus spp.*, a difference in spectra between healthy and diseased samples appeared at 1425 cm^{-1} . A peak at 2982 cm^{-1} in the spectrum from the healthy sample of citrus was absent from the spectrum of the diseased sample. The spectral marker for pentanone [17] is clearly present in the healthy citrus spectrum but is absent from the diseased spectrum. Work by Aksenov [16] found that pentanone was retained in healthy citrus plants but released when infected with Huanglongbing and corroborates the work carried out here. The cutin spectral marker in healthy *Pinus spp.* (Figure 3a) and healthy *Citrus spp.* (Figure 4a) has been clearly identified with reference to work by Dubis [19] and Heredia-Guerrero [20].

Future work will include making repeat measurements from each sample to corroborate the measurements reported here. A chemometric analysis will be carried out to clearly define infected spectra and healthy spectra. From this it will be possible to develop a computer algorithm for identifying infected and healthy samples.

6.0 Acknowledgments

The work was supported by the European Union Framework 7 project: Q-Detect, ‘Developing Quarantine Pest Detection Methods for use by National Plant Protection Organizations (NPPO) and Inspection Services’. The authors would like to thank Rebecca Lawson and Jennifer Hodgetts at the Food and Environment Research Agency for the plant preparations.

7.0 References

- [1] Strange, R.N., Scott, P.R., 2005 Plant Disease: A Threat to Global Food Security. *Annual Review of Phytopathology*. 43, pp. 83-116, (2012).
- [2] Dukes J.S., Pontius J., Orwig D., Garnas, J.R., Rodgers, V.L. Brazee, N. Cooke, B., Theoharides, K.A., Strange, E.E., Harrington, R., Ehrenfield, J., Gurevitch, J., Lerdau, M., Stinson, K., Wick, R., Ayres, M. Responses of insect pests, pathogens, and invasive plant species to climate change in the forests of northeastern North America: what can we predict? *Canadian Journal of Forest Research*. 39(2), 231–248. (2009).
- [3] Webber, J.F., Mullett, M., Brasier, C.M. Dieback and mortality of plantation Japanese larch (*Larix kaempferi*) associated with infection by *Phytophthora ramorum*. *New Disease Reports*. 22, pp. 19. (2010).
- [4] Redahan, E. Tackling larch enemies - genetic analysis of *Phytophthora ramorum*. *Wood Focus Magazine*.
- [5] Donald, P.A., Stamps, W.T., Linit. M.J. Pine wilt disease. *The Plant Health Instructor*. DOI:10.1094/PHI-I-2003-0130-01, (2003).
- [6] Curran, P.J. Remote Sensing of Foliar Chemistry. *Remote Sensing of Environment*. 30, pp. 271-278. (1989).
- [7] Warner, T.A., Duane E.M., Foody, G.M. (Eds), *The Sage Handbook of Remote Sensing*. (2009).
- [8] Widmer, T. L. Infective potential of sporangia and zoospores of *Phytophthora ramorum*. *Plant Disease*. 93:30-35. (2009).
- [9] Bertoluzza, A., Bottura. G., Lucchi, P., Marchetti, L., Zechini D'Aulerio, A. Molecular Monitoring of Horse Chestnut Leaves Affected With Biotic and Abiotic Disorders. *Journal of Plant Pathology*. 81 (2), 89-94. (1999).
- [10] Ivanova, D.G., Singh, B.R. Non-destructive FTIR monitoring of leaf senescence and elicitin-induced changes in plant leaves. *Biopolymers*. pp. 79–85. (2003).
- [11] Hawkins, S.A., Park, B., Poole, G.H. Gottwald, T., Windham, W.R., Lawrence, K.C. Detection of Citrus Huanglongbing by Fourier Transform Infrared-Attenuated Total Reflection Spectroscopy. *Applied Spectroscopy*. 64 (1). pp 100-103. (2010).

- [12] Hawkins, S.A., Park, B., Poole, G.H. Gottwald, T., Windham, W.R. Albano, J., Lawrence, K.C. Comparison of FTIR spectra between Huanglongbing (Citrus Greening) and other Citrus maladies. *J. Agric. Food Chem.* 58. pp 6007-1010. (2010)
- [13] Plešerová, L, Budínová, G., Havířova, K., Matějka, P. Skácel, F., Volka, K. Multivariate analysis of attenuated total reflection spectra of Norway Spruce Needles. *Journal of Molecular Structure.* 565-566, pp. 311-315, (2001)
- [14] Salman, A., Lapidot, I., Pomerantz, A., Tsrur, L., Hammody, Z., Moreh, R., Huleihel, M. Mordechai, S. Detection of *Fusarium oxysporum* Fungal Isolates Using ATR Spectroscopy. *Spectroscopy.* 27, 5-6, pp 551-556. (2012)
- [15] Zhang, Z.X., Liu, P., Kang, H.J., Liao, C.C., Pan C.C., Li, C.H., 2008. FTIR Spectra of Endangered Plants *Ulmus Elongata* and Its Correlation to Soil Nitrogen. *Spectroscopy and Spectral Analysis*, 6, pp. 1255-1259, (2008).
- [16] Aksenov, A.A., Pasamontes, A., Peirano, D.J., Zhao, W., Dandekar, A.M., Fiehn, O., Ehsani, R. Davis, C.E. Detection of Huanglongbing Disease using Differential Mobility Spectrometry. *Analytical Chemistry.* 86, pp. 2481-2488. (2014)
- [17] SDBSWeb: <http://sdfs.db.aist.go.jp> (National Institute of Advanced Industrial Science and Technology) (last accessed on 6/10/14)
- [18] Da Luz, B.R., Attenuated Total Reflectance Spectroscopy of Plant Leaves: a Tool for Ecological and Botanical Studies. *New Phytologist.* 172. pp 305-318. (2006).
- [19] Dubis, E.N., Dubis, A.T. Morzycki, J.W. Comparative analysis of plant cuticular waxes using HATR FT-IR reflection technique. *Journal of Molecular Structure.* 511-512. pp. 173-179. (1999)
- [20] Heredia-Guerrero, J.A. Benítez, J.J., Domínguez, E., Bayer, I.S. Cingolani, R., Athanassiou, A. Heredia, A. Infrared and Raman spectroscopic features of plant cuticles: a review. *Frontiers in Plant Science. Plant Biophysics and Modelling.* 5, 1-14, (2014).
- [21] Burkart, A., Cogliati, S., Rascher, U. Hyperspectral Reflectance Measurements Over Agricultural Crops By an UAV Based Ultra-Light Weight Microspectrometer. 2. Workshop Unbemannte Autonom fliegende Systeme (UAS) in der Landwirtschaft, Berlin, Deutschland, 05/06/2013 - 05/07/2013 Bornimer agrartechnische Berichte 81, 148 - 153 (2013).

- [22] Miyazaki, T., Plotto, A. Goodner, K. and Gmitter, F.G. Distribution of Aroma Volatile Compounds in Tangerine Hybrids and Proposed Inheritance. *J Sci. Food Agric.* 2011; 91: 449–460, (2010)
- [23] Trebolazabala J., Maguregui M, Morillas H, de Diego A, Madariaga J.M. Use of portable devices and Confocal Raman Spectrometers at Different Wavelength to Obtain the Spectral Information of the Main Organic Components in Tomato (*Solanum lycopersicum*) Fruits. *Spectrochim. Acta. A. Mol. Biomol. Spectrosc.* 105: 391-399. (2013)